Journal of Electroceramics 5:2, 141–152, 2000

Composite Electrodes in Solid Oxide Fuel Cells and Similar Solid State Devices

MOGENS MOGENSEN, SØREN PRIMDAHL, METTE JUHL JØRGENSEN & CARSTEN BAGGER
Materials Research Department, Risø National Laboratory, DK-4000 Roskilde, Denmark

Submitted January 4, 2000; Revised February 7, 2000; Accepted February 7, 2000

Abstract. The most important requirements to electrodes for solid oxide fuel cells and similar devices are listed, and it is explained how the requirements usually lead to a composite electrode. Three examples of composite electrodes are described in some details, namely the ceria based hydrogen electrode, the Ni-YSZ cermet anode and the LSM-YSZ. Here YSZ means yttria stabilized zirconia, and LSM is lanthanum strontium manganate.

Keywords: composite electrodes, electrode requirements, Ni-YSZ cermet, (La,Sr)MnO_3-YSZ composite, ceria anode, functional gradients, solid oxide fuel cell, high temperature steam electrolyzer

1. Introduction

Electrodes for solid oxide fuel cells (SOFC) are usually composite electrodes because the requirements to an SOFC electrode are so comprehensive that no single material is able to fulfil them. This is also generally the case for electrodes in a number of other electrochemical devices such as batteries, electrolysers, electrochemical pumps and sensors. However, the range of requirements is very much varying when the whole field of electrochemical technology is considered. This paper focuses on electrodes for the high temperature (600–1000°C) SOFC, but devices such as the solid oxide electrolysis cell (SOEC), electrochemical pumps and sensors have similar demands to the electrode properties. Common features of these devices are that they are all-solid-state gas electrodes (i.e., no liquid components), they operate at high temperatures, they have a ceramic ionic conductor as electrolyte, and they contain at least one ceramic component in both of the electrodes. This paper outlines the general requirements with emphasis on the SOFC electrodes. Two examples are treated in details, namely the Ni-YSZ-cermet SOFC *anode*, the negative electrode where the *oxidation* of the hydrogen takes place, and the LSM-YSZ-composite SOFC *cathode* (YSZ = yttria stabilized zirconia and LSM = lanthanum strontium manganate). The SOFC *cathode* is the positive electrode where the oxygen *reduction* takes place. Another electrode, the ceria based SOFC anode, is also briefly discussed as an example of a significantly different type of composite electrode.

2. Requirements to Electrodes

Several authors have dealt with the requirements to SOFC electrodes previously, e.g., [1–4]. Table 1 lists a set of electrode requirements. It should be noted that the required value of the specific electronic conductivity is dependent on the actual design of the fuel cell stack. The limit of 100 S/cm is only valid for the bipolar flat plate design. In other designs with long current paths in the electrode plane, a much higher value may be demanded. It is in principle possible to compensate a bad electronic conductivity with a thicker layer of electrode material, but the gas diffusion through thick layers of porous material may give rise to unacceptable diffusion polarisation as detailed below.

Probably, the highest demands are on the electrodes of the high temperature electrolyser (reversed SOFC) at least with respect to redox stability. The

Table 1. A list of requirements to a composite electrode in a commercially viable SOFC stack with operation temperatures in the range of 600 to 1000°C

Requirement	Technology/ Economy	Background/Comment
Dimensional and thermodynamical stability at relevant temperatures and P_{O_2}	Technology	Example: For the anode at 1000°C from 10^{-18} atm to 0.2 atm O_2
Good thermal expansion coefficient (TEC) matching with other stack materials	Technology	In particular to that of the load bearing structural element of the cell (or cell stack)
Good adhesion and electrical (ionic) contact to the electrolyte*	Technology	
Chemical compatibility with other cell and stack components	Technology	Both during cell fabrication (sintering), stack assembly and operation
Chemical compatibility with the gaseous reactants and products	Technology	
Polarization resistance $<0.1\,\Omega cm^2$	Economy	The stack price has an almost linear dependence on the polarization resistance
Electronic conductivity > 100 S/cm	Economy	To assure efficient current collection. The actual value is strongly design dependent
Tolerance to natural available fuels (SOFC anode)	Economy	To avoid expensive fuel cleaning
Cheap materials and applicability of a cheap fabrication process	Economy	To make the device commercially viable

*Anchoring to electrolyte and percolation through ionic and electronic conducting phases.

cathode, the negative electrode on which the *reduction* of water takes place must be stable at potentials down to -1.4 V versus O_2 (1 atm) in order to sustain a sufficiently fast hydrogen evolution rate. The *anode* (the positive electrode) must be stable up to $+0.3$ V versus O_2 (1 atm) to assure a high enough *oxidation* rate of oxide ions to oxygen gas. Both electrodes should be able to tolerate the gas from the other electrode through possible cracks and pinholes, and this is important in the SOEC as well as the SOFC mode.

However, other requirements may arise in specific applications. For instance, low temperature oxygen sensors need low electrode polarization resistances, i.e., the sum of the polarization resistances must be insignificant compared to the electronic resistance of the electrolyte. High temperature sensors such as for oxygen measurements in molten steel during steel production demand both high thermal shock resistance and chemical stability. The oxygen sensor used in combustion engines (the lambda sensor) must be resistant towards poisoning and interference by other gaseous components than oxygen.

Several types of composites may be exploited. The simplest type of composite electrode is a single layer containing a mixture of two phases with similar particle size. For SOFC electrodes the two phases would typically be the electrolyte (YSZ) and an electronic conducting electrode material. An example is the porous 10 to 50 μm thick Ni-YSZ electrode. In case of the LSM-YSZ cathode the porous composite electrode may have a too low lateral electronic conductivity. Therefore, it is necessary to add a current collector on top of it, e.g., a porous 50 μm thick layer of LSM [5–7]. Naturally, this may be done in a more sophisticated way by making functional gradients in order to induce the desired properties. Such gradients may be in both composition and in structure [8–10]. The limit in complexity will often be set by economics as a more sophisticated structure requires more advanced and expensive fabrication methods. An example is the electrochemically very efficient ''tree-structured'' composite SOFC cathode developed by Osaka Gas using electrochemical vapour deposition (ECVD) [11,12], which may be too expensive for a technical device.

3. Examples of Composite Electrodes

The performance of a composite electrode naturally depends on the properties of the components, but it is

also very dependent on the details of the geometrical structure and the interaction between components. This is illustrated in the following using the composite hydrogen electrode, Ni-YSZ, and the composite oxygen electrode, LSM-YSZ, both on YSZ electrolytes as these are the most commonly used SOFC electrodes. Their properties, merits and shortcomings are described based on the requirements listed in Table 1. It should be noted that in order to get high and reliable performance of an SOFC stack these requirements must be fulfilled at any local operation conditions. Inherently, local conditions such as temperature and P_{O_2} will vary over wide ranges during operation, but also through the cell stack and laterally over the single cells at a given steady state stack operation condition.

In spite of the differences in materials and the types of processes taking place, the Ni -YSZ and the LSM - YSZ electrodes have a number of features in common. The reason for this is the composite nature of the electrodes with the electrochemical reactions taking place in zones near the three phase boundary (TPB) line (see Fig. 1). However, before looking into the details of these most widely investigated electrodes, let us have a look at the on-going development of a doped ceria electrode. This development started as an attempt of making a simple electrode using a mixed ionic and electronic conductor.

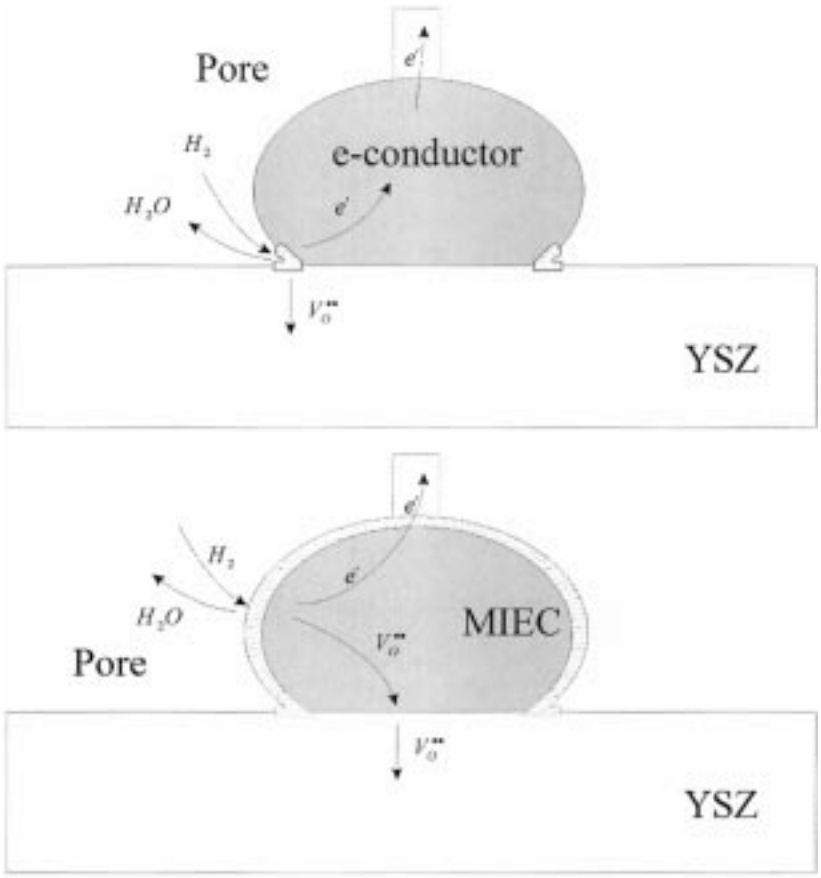

Fig. 1. Illustration of the difference in location of the electrode reaction on two SOFC electrode types. Upper: In an electrode where the electrode material is exclusively an electronic conductor, the reaction zone is restrained to the vicinity of the triple phase boundary (TPB). Lower: In a mixed ionic-electronic conductor (MIEC) the electrode reaction can take place on the entire electrode surface.

3.1. The Doped Ceria Electrode with Mixed Conductivity

A simple electrode design would appear to involve only a single material, but it is very difficult to find one material, which will fulfil all the requirements of Table 1. For instance, the requirement for a low electrode polarisation resistance points to the use of a mixed conductor with electronic and ionic conductivity in order to get as high active electrode area as possible as illustrated in Fig. 1. Takahashi et al. [13] showed that doped ceria is an excellent hydrogen electrode at 1000°C and explained this to be due to the mixed ionic and electronic conductivity of reduced ceria. However, ceria undergoes a change of volume when the oxygen partial pressure P_{O_2} is varied. Furthermore, the electronic conductivity of doped ceria is not sufficient to take care of the current collection in an SOFC stack [4], and the sintering of a doped ceria anode on a YSZ electrolyte involves formation of a reaction (diffusion) zone with limited oxide ion conductivity [14,15].

The ceria expansion and reaction problems may be minimized by a composite solution where YSZ particles protrude into the ceria layer at short distances for anchoring, providing sufficient adhesion at low sintering temperature [16]. Sintering of the ceria on YSZ at temperatures below about 1200°C prevents any significant diffusion of ceria and YSZ into each other. To limit the mechanical implications of the volume instability during redoxing, the ceria layer must be thin. This makes the problem of the low electronic conductivity even worse, and therefore, it is necessary to add a current collection layer of another material with high electronic conductivity [16]. A sketch of this kind of advanced composite is shown in Fig. 2.

It appears that instead of a simple electrode a complicated one emerged, and a suitable (cheap and redox stable) current collector material has not yet been demonstrated. Nevertheless, ceria based anodes have important advantages over conventional Ni-based anodes, namely the ability to endure repetitive oxidation and reduction (redoxing) and the ability to avoid (or tolerate) carbon deposition from hydrocarbon fuels. These properties strongly encourage continued efforts of developing this electrode.

3.2. The Ni-YSZ Electrode

Variables which may be used for controlling the properties of Ni-YSZ-electrodes are: (1) Ni/YSZ volume ratio, and (2) porosity and particle size distribution which is mainly affected by raw materials morphology, application methods and production parameters such as milling and sintering. In the following the various electrode properties are mainly related to these parameters, as they are the only ones studied systematically so far. The effect on the properties of the composite of other parameters such as doping the YSZ with other oxides or alloying the Ni with other metals have not yet been studied to any appreciable extent.

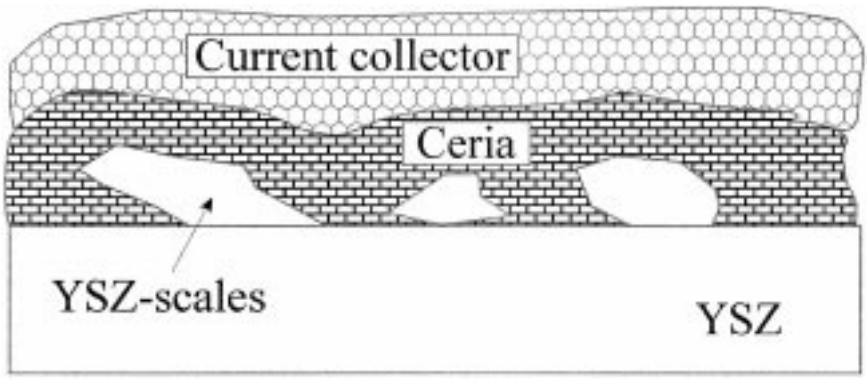

Fig. 2. Electrode structure with two elements of composite structure. (1) The electrode adhesion on the interface towards the dense electrolyte is improved by a physical anchoring (YSZ-scales), and (2) the electrode functions are divided on two layers taking care of the electrochemical conversion (ceria) and current collection, respectively.

3.2.1. Electrode mechanism and polarization resistance. Ni is a very good bond breaker of both the H-H and the C-H bond in CH_4 [17]. In spite of this, the polarization resistance, R_P, is unacceptably high for a pure Ni electrode. At temperatures of 800 to 1000°C pure nickel metal has a high surface mobility [18], causing it to sinter and agglomerate into a coarse structure with a limited TPB against the electrolyte surface. In a composite with the electrolyte material a substantially longer TPB can be obtained per unit area of cell, provided that two interwoven solid networks of the two phases are obtained to provide TPB's throughout the electrode volume. In this composite structure Ni particles tend to sinter and grow until the YSZ network confines them and thus prevents them from further growth. This means that the structure of the YSZ network controls the total structure of the composite including the structure of the porosity as sketched in Fig. 4. So far there seems to be general agreement about this in the literature. It is also agreed that the longer the TPB-length per unit cell area the lower is the polarization resistance [19,20].

In order to optimize the Ni-YSZ structure, knowledge about the type of process which limits R_P is needed. The value of the TPB line specific resistance should be known and preferably also the widths of the reaction zones on the Ni and on the YSZ along the TPB as well as the spatial distribution of the current densities within these zones. If this information is available, the optimal structure and thickness of the cermet may be calculated using statistical models [21]. However, there are discrepancies in literature.

Possible reaction paths are suggested in Fig. 3. The type of processes have been discussed in some details

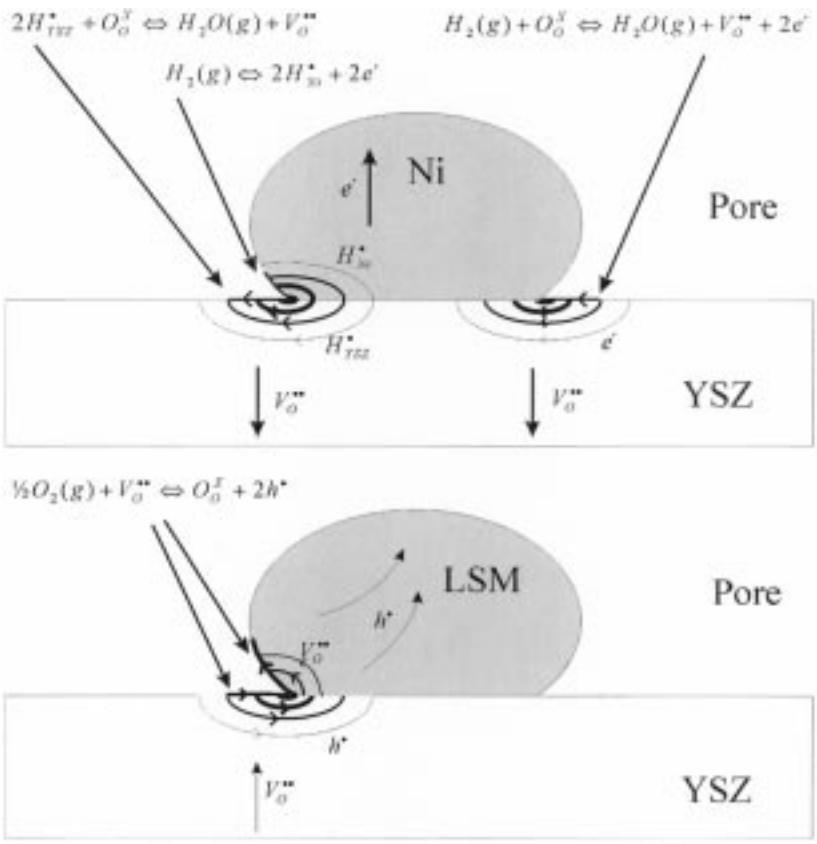

Fig. 3. Possible reactions in SOFC electrodes near the TPB. Upper: Anodic reactions in the $H_2/H_2O/Ni/YSZ$ electrode, to the left including bulk transport of H^+ in Ni and YSZ, to the right including bulk transport of electrons in YSZ. Lower: Cathodic reactions in the air/LSM/YSZ electrode, including bulk transport of holes in YSZ and oxide vacancies in LSM.

[22–27]. The charge transfer may partly take place at the electrolyte surface because the YSZ electrolyte has some electronic conductivity [28,29], which is probably very dependent on trace impurities. Also NiO is slightly soluble in YSZ. The solubility varies with temperature from about 1.1% at 1200°C to about 1.7% at 1600°C [30,31]. A solubility around 0.5% at 800°C is found by extrapolation. In the reducing fuel atmosphere Ni metal will precipitate in the YSZ.

As discussed previously [24,32,33], it is reasonable to assume a significant degree of hydrogen coverage on the Ni even at 1000°C. Also hydrogen (protons) is slightly soluble in Ni (6×10^{-4} atom %) and highly mobile. The diffusion coefficient is 1.5×10^{-4} cm^2/s at 1000°C. Finally, protons are to a low extent soluble and mobile in the YSZ (proton concentration up to about 2×10^{-5} atom% and diffusion coefficient 1×10^{-6}cm^2/s). This seems to be enough to allow local current densities of protons through the bulk YSZ of the order of 100 mA/cm^2 at distances of up to 1 μm from the Ni [24]. Thus, it seems that the hydrogen oxidation (and water reduction) may proceed through a number of consecutive steps and through different parallel paths, and in fact evidence of entirely different rate limiting steps at temperatures below 845°C and above 890°C has been presented [26].

Experimental evidence exists, which indicate that the reaction zone width on Ni is less than 1 μm [34]. The extension of the electrode process onto the YSZ surface is not well determined, but a value of no more than 13 μm at 700°C has been indicated based on experiments with Ni pattern electrodes [35].

As the specific electronic conductivity of Ni is orders of magnitude higher than the specific ionic conductivity of YSZ, the electrochemical active volume is expected to reside near to the electrolyte surface. The distance from the YSZ electrolyte surface into the cermet where the electrochemical reactions take place is called the active thickness. It has been found to be about 10 μm at 1000°C [36,37] as shown in Fig. 5(a).

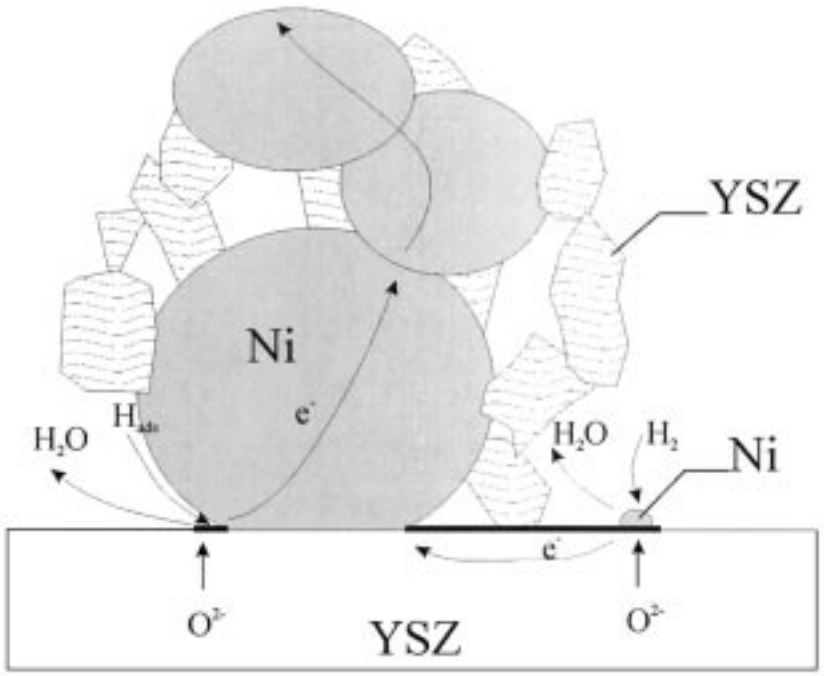

Fig. 4. Sketch of Ni-YSZ cermet anode. To the left hydrogen oxidation at the TPB of connected Ni-particles, to the right hydrogen oxidation at an isolated Ni-particle requiring electronic conductivity of the YSZ to participate in the reaction. Connected Ni-particles are known to agglomerate and grow until the YSZ-network surrounding them prevents further growth.

The lowest reported values of polarization resistance, R_P, for the H_2/H_2O/Ni-YSZ electrode are about 20 to 40 $m\Omega cm^2$ at 1000°C [38]. No details of the anode fabrication procedure were given. At Risø the status of the Ni-YSZ electrode is $30 m\Omega cm^2 < R_P < 60 m\Omega cm^2$ at 1000°C and $60 m\Omega cm^2 < R_P < 120 m\Omega cm^2$ at 850°C for anodes produced by spray painting. The fabrication details are described elsewhere [10,39,40].

3.2.2. Lateral electronic conductivity. Here the current collection structure is treated as a part of the electrode even though this approach may be discussed. In order to keep the internal resistance of the SOFC stack low it is necessary to have an efficient current collector. For the bipolar flat plate design a typical lateral current path length of about 1 mm can be assumed. If the resistive contribution should be negligible, say less than $10 m\Omega cm^2$ for a 200 μm thick 30% porous structure, this implies a specific electronic conductivity of about 100 S/cm. Other cell designs containing substantially longer lateral current paths in the electrodes may need a much higher specific conductivity, as the conductivity cannot just be overcome by a thicker electrode due to gas diffusion limitations [41,42]. To illustrate this point the diffusion resistance of a porous layer of 1 mm thickness is estimated to $50 m\Omega cm^2$ [43,44]. This is 50% of the acceptable polarization. The assumption for this calculation was: the porosity is 30%, the pores are larger than 1 μm, i.e., no Knudsen diffusion, and the tortuosity factor is 3.

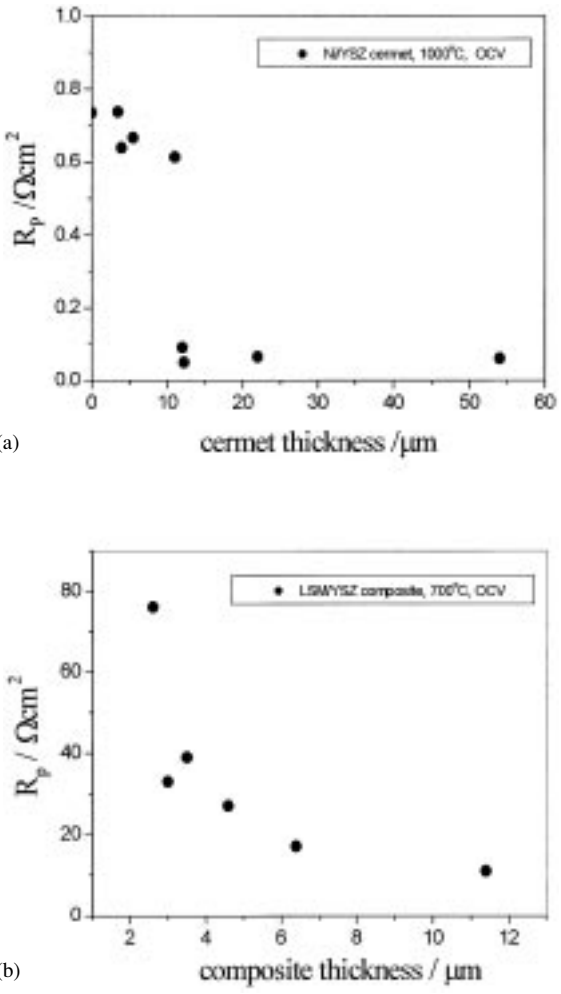

Fig. 5. Active thickness of composite electrodes produced by spray painting and sintering at 1300°C. (a) Ni-YSZ cermet anodes with 40 vol % Ni [37]. (b) LSM-YSZ composite cathodes with 50 wt % LSM [6].

The electronic conductivity of a simple Ni-YSZ cermet structure with randomly mixed particles of similar size seems to follow the rules of percolation with a fair approximation [45,46]. This means that gradually varying the Ni content from below 30 vol % of solids to above 50 vol %, there is an abrupt increase in the electronic conductivity. The inflexion point of the S-shaped curve is in the range of 30–40 vol % Ni. If a significant fraction of the YSZ particles are much bigger that the Ni particles then the inflexion point may be moved down to 15 vol % Ni [47]. However, in order to get a long TPB length, a significant amount (20–30%) of the YSZ must have very fine particles, below 1 μm diameter, at least in the vicinity of the electrolyte. Fine YSZ particles must be evenly distributed around the Ni-particles in order to keep both a stable TPB length and electronic conductivity over long periods of time. Otherwise the Ni particles will grow and become too coarse. The porosity of the simple cermet with 40 vol % Ni (of the solids) must be lower than about 30–35% after the reduction of the NiO to Ni [48,49]. Otherwise the connectivity between the Ni-particles is lost.

3.2.3. Dimensional and thermodynamic stability. The durability of anode performance is to a large extent linked to the microstructure in the same way as attainable performance. For a cermet with coarse and fine YSZ sintered together with NiO, a negligible degradation over 2500 h at 1000°C with $200 mA/cm^2$ has been demonstrated [50]. For cells with a Ni-YSZ

cermet fabricated by fixation of the Ni metal using electrochemical vapour deposition of YSZ under reducing conditions no measurable degradation was found over 4800 h at 1000°C with 450 mA/cm^2 and a fuel utilization of 85% [51].

Accidental oxidation of the Ni-YSZ cermet anode is generally found to be detrimental. The volume expansion of the Ni metal by oxidation to NiO typically leads to destruction of the surrounding YSZ framework. The molar volume of Ni and NiO is 6.6 cm^3/mol and 11.1 cm^3/mol, respectively.

The stability of Ni in the anode is affected by high water vapor pressures at operation temperatures. $Ni(OH)_2$ has been calculated to have a significant vapor pressure at high pH_2O, and depletion of Ni from cermet anodes at the gas inlet has been demonstrated in durability tests [52]. The gradients in pH_2O at active TPB's are supposed to be responsible for this Ni dissolution and a following deposition elsewhere as the pH_2O decreases and the $Ni(OH)_2$ decomposes.

3.2.4. Thermal expansion coefficient matching. The difference in thermal expansion coefficient (TEC) between the electrolyte and the Ni-YSZ cermet electrode layers and the resulting stress buildup must also be considered. The TEC of TZ8Y is between $10.6–11.0 \times 10^{-6}\,K^{-1}$ [53]. A TEC of $14 \times 10^{-6}\,K^{-1}$ can be found for NiO, and a TEC of $12.3 \times 10^{-6}\,K^{-1}$ can be measured for a NiO/YSZ composite with 53 vol % NiO [54], i.e., about what would be found by linear interpolation between the values of the two components. For a Ni-YSZ cermet with 40 vol % Ni the TEC value was found to be close to that of YSZ. This seems low considering the TEC of pure Ni is about $17 \times 10^{-6}\,K^{-1}$. The reason is that the elastic modulus of Ni is only in the range of 14.8–21.1 GPa compared to 137–157 GPa for YSZ [54]. This means that if a well sintered YSZ network is established this will control the measured overall TEC of the cermet, but it may cause a build-up of internal stresses.

The non-reduced NiO-YSZ composite has a TEC which is close to the weighted average of the TECs of the two components because the eleastic modulii of the two oxides are approximately equal [54]. Considering cells to be stress free at the sintering temperature of 1300–1350°C in air, the TEC difference between the composite and the YSZ causes tensile stresses in the composite at lower temperatures. This may result in serious crack formation in the composite and these cracks may proceed into the electrolyte sheet causing cell failure during cool down [55].

3.2.5. Chemical compatibility with stack components and gaseous reactants. In general the Ni-YSZ cermet is very stable towards other stack components. No detrimental reactions are detected for silica based glass seals in contact with the cermet, whereas Ni-depletion by nickel-phosphate formation is observed by reaction with phosphate based glasses [56]. Sulphur and sulphur compounds known to reside in natural fuels are also known to adsorb to the Ni-surface and to cause a loss of electrode performance. This effect is similar to catalytic poisoning, and is in some cases observed to be reversible [57].

As mentioned in Table 1 the SOFC anode should be able to tolerate natural available fuels without expensive fuel cleaning. In this respect Ni is far from ideal. If it is exposed to pure methane or other hydrocarbons at SOFC operating temperatures, the hydrocarbons will crack forming hydrogen and carbon because Ni is a good cracking catalyst [17]. Unfortunately, carbon dissolves in Ni causing a volume expansion. Furthermore, if the carbon activity is high enough the carbon tends to precipitate on the interface between the Ni and the YSZ. Thus, the Ni-cermet is both chemically and mechanically destroyed by hydrocarbons. The way around this is steam reforming, either external or internal. In the latter case, the reforming takes place on the Ni in the cermet electrode, and this causes another problem. At high temperatures the reforming reaction may be very fast, and the reforming reaction is strongly endothermic. This causes steep temperature gradients, which may result in mechanical failure of the cell [58].

3.3. The LSM-YSZ Electrode

Variables which may be used for controlling the properties of LSM-YSZ-electrodes are: (1) LSM/YSZ volume ratio, (2) stoichiometry of the LSM, i.e., the (La + Sr)/Mn-ratio and the La/Sr-ratio, (3) porosity and particle size distribution which is mainly affected by the properties of the starting powders, the application methods, and production parameters such as milling time and sintering temperature.

3.3.1. Polarization resistance. Possible reaction paths for the oxygen reduction at the LSM-YSZ electrode are shown in Fig. 3(b). It is uncertain to which extent diffusion of oxygen in the LSM phase is a limiting factor, but the oxide ion conductivity of LSM is known to be low [59]. This restricts the electrochemical processes to take place at or near the TPB. This is in line with the finding that the oxygen electrode reaction rate is essentially proportional to the length of the TPB for porous (not composite) doped lanthanum manganate electrodes at small overpotentials [60]. Thus, the way of optimizing the LSM cathode should be through an LSM-YSZ composite electrode, and this point has been well proven [5–7,61,62]. The active thickness of a 50/50 wt % LSM/YSZ composite electrode sintered at 1300°C is found to be about 10–15 μm in the temperature range of 700 to 1000°C [6], see Fig. 5(b).

The detailed reaction mechanism for the oxygen reduction on an LSM/YSZ electrode is not well understood. From experiments with pointed electrodes the width of the reaction zone on the YSZ is indicated to be no more than a few microns [32]. The TPB length-specific resistance is in the range from about 750 Ωcm for undoped lanthanum manganate electrodes to about 20 Ω cm for 50% Sr substitution on the La sites (in air at 1000°C at -75 mV overpotential). The actual values are very much dependent on the detailed history of the electrode, i.e., of the current density and the time with the current density of a given magnitude [63–66].

The status at Risø is that the polarisation resistances of the LSM-YSZ composite air electrode is $30\,\mathrm{m\Omega\,cm^2} < R_P < 50\,\mathrm{m\Omega\,cm^2}$ at 1000°C and $70\,\mathrm{m\Omega\,cm^2} < R_P < 120\,\mathrm{m\Omega\,cm^2}$ at 850°C. It is essential to sinter the electrodes at a temperature of about 1100°C and also a functional grading of the composite electrode seems to be important in order to obtain high performance [10,67].

3.3.2. Lateral electronic conductivity. The composite LSM-YSZ-layer has a far too low conductivity to take care of the current collection. As pure LSM possesses a reasonably high electronic conductivity in the range of 50–350 S/cm at temperatures of 700–1000°C depending on Sr concentration and temperature [68,69] it may be used for current collectors if it is sintered properly. This may require sintering temperatures of about 1300°C. This may in turn be a problem in certain designs where the current collector must be sintered below 1100°C due to the sensitivity to high temperatures of the underlying composite electrode. In such cases the in-plane conductivity may be low because of high porosity and because of a limited particle-neck formation between the LSM particles in the current collecting layer. The conductivity may be improved by substituting 50% or more of the Mn in $La_{1-u}Sr_uMnO_3$ with Co. However, this increases reactivity and TEC mismatch with YSZ [70] as explained in more details below.

The gaseous oxygen diffusion limitation may be significant for the air electrodes, as the diffusion coefficient for oxygen in nitrogen is substantially smaller than for water in hydrogen [41]. An appreciable diffusion resistance may be the result, especially for a case like the Siemens-Westinghouse cell design with a 2.2 mm thick porous cathode support [38,71].

3.3.3. Dimensional and thermodynamic stability. The oxygen/manganese (O/Mn) ratio of $La_{1-u}Sr_uMnO_{3\pm\delta}$ varies considerably with P_{O_2}, temperature, degree of strontium doping, and (La + Sr)/Mn-ratio. The O/Mn ratio ranges from 3.18 in pure oxygen at 600°C, to about 2.75 in atmospheres with $P_{O_2} < 10^{-15}$ atm at 1000°C for a Sr doping of 30%. $La_{1-u}Sr_uMnO_3$ is unstable in very reducing atmospheres such as the anode gas at 1000°C. It splits up into La_2O_3, MnO, $SrMnO_3$ and $La_2Mn_2O_4$ when the O/Mn ratio goes below about 2.8, i.e., the decomposition starts in the range $10^{-15}\,\mathrm{atm} < P_{O_2} < 10^{-14}$ atm at 1000°C slightly dependent on the exact composition of the LSM [72–74]. The lanthanum manganate crystal unit cell volume may change up to 5% due to stoichiometry changes [75,76], and also other properties of the LSM change with stoichiometry [77]. At high oxygen partial pressures the lattice contains cation vacancies which provides the charge compensation for the Mn^{4+} formed at high P_{O_2}. This means, fortunately, that the change in molar volume is much less than the change in unit cell volume because the number of unit cells per mol also changes when P_{O_2} changes.

3.3.4. Thermal expansion coefficient matching. The TEC of LSM materials increases with the Sr-content from ca. $11.2 \times 10^{-6}\,\mathrm{K^{-1}}$ for zero Sr content to ca. $13 \times 10^{-6}\,\mathrm{K^{-1}}$ for 50% Sr doping [69,78], but discrepancies exist in the literature [69,79]. This may be due to differences in measurement procedures

and actual measured temperature ranges. The figures given here are averaged over the temperature range from room temperature to 1000°C or 1100°C. Also, it should be noted that LSM may undergo phase transitions upon heating, cooling or change in P_{O_2} [75,80]. This is unwanted because a phase transition is associated with a volume change which may degrade the composite electrode.

In order to enhance the lateral electron conductivity of the current collecting layers and to widen the TPB, partial substitution of Mn with Co has been proposed because both the electronic and the ionic conductivity of strontium doped lanthanum cobaltites (LSCo) are orders of magnitudes higher than those of the LSM. However, the reactivity between LSCo and YSZ is severe, and the TEC of $22 \times 10^{-6}\,K^{-1}$ is excessive compared to $10.8 \times 10^{-6}\,K^{-1}$ for YSZ. Therefore, a gradual change from YSZ over LSM to the pure LSCo is necessary [70], but the economic feasibility of such a complicated electrode structure is uncertain.

3.3.5. Chemical compatibility with the YSZ electrolyte. If the LSM is put into close contact with YSZ, reactions may take place at temperatures above 900°C within times less than 1000 h. The LSM is in fact stable towards YSZ as long as the activity of La_2O_3 or SrO is low [81], but if no precautions are taken MnO_x will diffuse from the LSM phase into the YSZ leaving ''free'' La_2O_3 or SrO, which immediately reacts with YSZ forming poorly conducting $La_2Zr_2O_7$ or $SrZrO_3$ [5,81–87]. One way around the problem is to have an Mn-over-stoichiometry in the LSM of a few %, enough to saturate the YSZ without forming ''free'' La_2O_3 or SrO. A Sr substitution between 20 and 40% also helps to avoid formation of reaction products at the YSZ-LSM interface. Dissolution of MnO_x in the YSZ lattice causes a decrease in the oxide ion conductivity by roughly a factor of 5 at 800°C and an increase in the activation energy from ca. 0.9 eV to ca. 1.2 eV [81].

4. Concluding Remarks

The performance of composite SOFC electrodes in terms of area-specific polarisation resistance is at present suitable for technological exploitation using ''classical'' materials such as Ni-YSZ and LSM-YSZ. However, there is still room for improvements especially at temperatures lower than 850°C. Materials with a broader stability range in terms of P_{O_2} are wanted for both electrodes, and especially ceria with a suitable catalyst and a redox-stable current collector structure may contribute to the development of an electrode for natural gas conversion and electrolyzer operation. During this development it should be born in mind that the materials and fabrication processes should be cheap. Fabrication processes such as tape casting, calendering, spray painting are cheap and suited for mass production. Finally it should be noted that for SOFC a lifetime of 40.000 h with a degradation rate of less than 0.5% per 1000 h is required in order to make power generation using SOFC competitive.

References

1. C.S. Tedmon, H.S. Spacil, and P. Mitoff, *J. Electrochem. Soc.*, **116**, 1170 (1969).
2. B.C.H. Steele, *J. Power Sources*, **49**, 1 (1994).
3. N.Q. Minh and T. Takahashi, *Science and Technology of Ceramic Fuel Cells* (Elsevier Science B.V., Amsterdam NL, 1995), ch. 5 and 6.
4. M. Mogensen, T. Lindegaard, U.R. Hansen, and G. Mogensen, *J. Electrochem. Soc.*, **141**, 2122 (1994).
5. M.J.L. Østergaard, C. Clausen, C. Bagger, and M. Mogensen, *Electrochim. Acta*, **40**, 1971 (1995).
6. M. Juhl, S. Primdahl, C. Manon, and M. Mogensen, *J. Power Sources*, **61**, 173 (1996).
7. M. Juhl, S. Primdahl, and M. Mogensen, in *High Temperature Electrochemistry: Ceramics and Metals* eds. F. W. Poulsen, N. Bonanos, S. Linderoth, M. Mogensen, and B. Zachau-Christiansen (Risø National Laboratory, Roskilde DK, 1996), p. 295.
8. K. Sasaki, P. Bohac, and L. J. Gauckler, in *Solid Oxide Fuel Cells III* edited by S. C. Singhal, H. Iwahara (The electrochemical Society, Pennington NJ, 1993), p. 288.
9. K. Sasaki and L.J. Gauckler, in *Proc. Int. Symp. Structural Functionally Graded Materials*, **3**, 651 (1995).
10. C. Bagger, S. Linderoth, M. Mogensen, P.V. Hendriksen, B. Kindl, S. Primdahl, P.H. Larsen, F.W. Poulsen, N. Bonanos, and M.J. Jørgensen, in *Solid Oxide Fuel Cells (SOFC VI)*, eds. S.C. Singhal and M. Dokiya, Proc. Vol. 99-19 (The Electrochemical Society, 1999), p. 28.
11. M. Suzuki, H. Sasaki, A. Kajimura, E. Yagasaki, and M. Ippomatsu, *J. Electrochem. Soc.*, **141**, 1928 (1994).
12. H. Sasaki, M. Susuki, T. Sogi, A. Kajimura, and E. Yagasaki, in *Solid Oxide Fuel Cells IV*, eds. M. Dokiya, O. Yamamoto, H. Tagawa, and S.C. Singhal (The Electrochemical Society, Pennington NJ, 1995), p. 187.
13. T. Takahashi, H. Iwahara, and Y. Suzuki, in *Proc. Third International Symposium on Fuel Cells* Bruxelles 16-20, VI (Presses Academiques Europeennes, Bruxelles B 1969), p. 113.

14. J.J. Bentzen and H. Schwartzback, *Solid State Ionics*, **40/41**, 942 (1990).
15. C. Clausen, *Electron Microscopical Characterisation of Interfaces in SOFC Materials*. PhD-thesis, Risø-R-626(EN) (1992).
16. O. Marina, C. Bagger, S. Primdahl, and M. Mogensen, *Solid State Ionics*, **123**, 199 (1999).
17. J.R. Rostrup-Nielsen, *Catalytic Steam Reforming* (Springer Verlag, Berlin, 1984).
18. M.M. Murphy, J. Van Herle, A.J. McEvoy, and K.R. Thampi, *J. Electrochem. Soc*., **141**, L94 (1994).
19. J. Mizusaki, H. Tagawa, T. Saito, K. Kamitani, T. Yamamura, K. Hirano, S. Ehara, T. Takagi, T. Hikita, M. Ippommatsu, S. Nakagawa, and K. Hashimoto, *J. Electrochem. Soc*., **141**, 2129 (1994).
20. T. Norby, O.J. Velle, H. Leth-Olsen, and R. Tunold, in *Solid Oxide Fuel Cells III*, eds. S. C. Singhal and H. Iwahara (The Electrochemical Society, Pennington NJ, 1993) p. 473.
21. S. Sunde, *J. Electrochem. Soc*., **143**, 1930 (1996).
22. E.J. Schouler and M. Kleitz, *J. Electrochem. Soc*., **134**, 1045 (1987).
23. J. Mizusaki, H. Tagawa, T. Saito, T. Yamamura, K. Kamitani, K. Hirano, S. Ehara, T. Takagi, T. Hikita, M. Ippommatsu, S. Nakagawa, and K. Hashimoto, *Solid State Ionics*, **70/71**, 52 (1994).
24. M. Mogensen, S. Sunde, and S. Primdahl, in *High Temperature Electrochemistry: Ceramics and Metals*, eds. F.W. Poulsen, N. Bonanos, S. Linderoth, M. Mogensen, and B. Zachau-Christiansen (Risø National Laboratory, Roskilde DK, 1996), p. 77.
25. P. Holtappels, L.G.J. de Haart, and U. Stimming, *J. Electrochem. Soc*., **146**, 1620 (1999).
26. P. Holtappels, I.C. Vinke, L.G.J. de Haart, and U. Stimming, *J. Electrochem. Soc*., **146**, 2976 (1999).
27. S. Primdahl, *Nickel/yttria-stabilised zirconia cermet anodes for solid oxide fuel cells*. PhD-thesis, University of Twente, 1999, Risø-R-1137 (EN).
28. J.-H. Park and R.N. Blumenthal, *J. Electrochem. Soc*, **136**, 2867 (1989).
29. H.L. Tuller, in *Nonstoichiometric Oxides*. ed. O.T. Sørensen (Academic Press, 1981).
30. S. Linderoth and A. Kuzjukevics, in *Solid Oxide Fuel Cells V*, eds. U. Stimming, S.C. Singhal, H. Tagawa, and W. Lehnert (The Electrochemical Society, Pennington, NJ, 1997), p. 1076.
31. A. Kuzjukevics and S. Linderoth, *Solid State Ionics*, **93**, 255 (1997).
32. M. Mogensen and S. Skaarup, *Solid State Ionics*, **86–88**, 1151 (1996).
33. S. Skaarup, B. Zachau-Chistiansen, and T. Jacobsen, in *High Temperature Electrochemistry: Ceramics and Metals*, eds. F.W. Poulsen, N. Bonanos, S. Linderoth, M. Mogensen, and B. Zachau-Christiansen (Risø National Laboratory, Roskilde DK, Denmark, 1996), p. 432.
34. N. Nakagawa, H. Sakurai, K. Kondo, T. Morimoto, K. Hatanaka, and K. Kato, *J. Electrochem. Soc*., **142**, 3474 (1995).
35. J. Mizusaki, T. Yamamura, N. Mori, H. Tagawa, K. Hirano, S. Ehara, T. Tagaki, M. Hishinuma, H. Sasaki, T. Sogi, Y. Nakamura, and K. Hashimoto, in *High Temperature Electrochemistry: Ceramics and Metals*, eds. F.W. Poulsen, N. Bonanos, S. Linderoth, M. Mogensen, and B. Zachau-Christiansen (Risø National Laboratory, Roskilde DK, Denmark, 1996), p. 363.
36. S. Sakamoto, H. Taira, and H. Takagi, *Denki Kagaku*, **64**, 609 (1996).
37. M. Brown, S. Primdahl, M. Mogensen, and N. Sammes, *J. Aust. Cer. Soc*., **34**, 248 (1998).
38. S.C. Singhal in *Solid Oxide Fuel Cells V*, eds. U. Stimming, S.C. Singhal, H. Tagawa, and W. Lehnert, Proc. Vol. 97-40 (The Electrochemical Society, Pennington NJ, 1997), p. 37.
39. C. Bagger, in *1992 Fuel Cell Seminar* (Courtesy Associates, Inc., Washington D.C., 1992), p. 241.
40. S. Primdahl, C. Bagger, M.J. Jørgensen, M. Mogensen, and O. Marina, patent pending (1998).
41. K.-Z. Fung and A.V. Virkar, in *Solid Oxide Fuel Cells IV*, eds. M. Dokiya, O. Yamamoto, H. Tagawa, and S.C. Singhal, (The Electrochemical Society, Pennington NJ, 1995), p. 1105.
42. J.-W. Kim, A.V. Virkar, K.-Z. Fung, K. Metha, and S.C. Singhal *J. Electrochem. Soc*., **146**, 69 (1999).
43. S. Primdahl and M. Mogensen, *J. Electrochem. Soc*., **146**, 2827 (1999).
44. M. Mogensen, P.H. Larsen, P.V. Hendriksen, B. Kindl, C. Bagger, and S. Linderoth, in *Solid Oxide Fuel Cells (SOFC VI)*, eds. S.C. Singhal and M. Dokiya, Proc. Vol. 99-19 (The Electrochemical Society, 1999), p. 904.
45. M.J. Powell, *Phys. Rev. B*, **20**, 10 (1979).
46. D.W. Dees, T.D. Claar, T.E. Easler, D.C. Fee, and F.C. Mrazek, *J. Electrochem. Soc*., **134**, 2141 (1987).
47. H. Itoh, T. Yamamoto, M. Mori, T. Horita, N. Sakai, H. Yokokawa, and M. Dokiya, *J. Electrochem. Soc*., **144**, 641 (1997).
48. M. Mogensen, S. Primdahl, J.T. Rheinländer, S. Gormsen, S. Linderoh, and M. Brown, in *Solid Oxide Fuel Cells IV*, eds. M. Dokiya, O. Yamamoto, H. Tagawa, and S.C. Singhal (The Electrochemical Society, Pennington NJ, 1995), p.657.
49. M.S. Brown, N.M. Sammes, and M. Mogensen, in *Solid Oxide Fuel Cells V* edited by U. Stimming, S.C. Singhal, H. Tagawa, and W. Lehnert, Proc. Vol. 97-40 (The Electrochemical Society, Pennington NJ, 1997), p. 861.
50. H. Itoh, T. Yamamoto, M. Mori, T. Watanabe, and T. Abe, *Denki Kagaku*, **64**, 549 (1996).
51. S.C. Singhal, in *High Temperature Electrochemistry: Ceramics and Metals*, eds. F.W. Poulsen, N. Bonanos, S. Linderoth, M. Mogensen, and B. Zachau-Christiansen (Risø National Laboratory, Roskilde DK, Denmark, 1996), p. 123.
52. A. Gubner, H. Landes, J. Metzger, H. Seeg, and R. Stübner, in *SOFC V,* eds. U. Stimming, S.C. Singhal, H. Tagawa, and W. Lehnert (The Electrochemical Society, Pennington NJ 1997), p. 844.
53. R. Männer, E. Ivers-Tiffée, and W. Wersing, in *Solid Oxide Fuel Cells (SOFCII),* eds. F. Grosz, P. Zegers, S.C. Singhal, and O. Yamamoto (Commission of the European Communities, Luxemburg, L. EUR-13564-EN, 715, 1991).
54. M. Mori, T. Yamamoto, H. Itoh, H. Inaba, and H. Tagawa, *J. Electrochem. Soc*., **145**, 1374 (1998).
55. B.F. Sørensen and S. Primdahl, *J. Mater. Sci*., **33**, 5291 (1998).

56. P.H. Larsen, S. Primdahl, and M. Mogensen, in *High Temperature Electrochemistry: Ceramics and Metals*, eds. F.W. Poulsen, N. Bonanos, S. Linderoth, M. Mogensen, and B. Zachau-Christiansen (Risø National Laboratory, Roskilde DK, Denmark, 1996), p. 331.
57. S. Primdahl and M. Mogensen, in *Solid Oxide Fuel Cells (SOFC VI)* Eds. S.C. Singhal and M. Dokiya, Proc. Vol. 99-19 (The Electrochemical Society, 1999), p. 530.
58. P.V. Hendriksen, in *SOFC V* Eds. U. Stimming, S.C. Singhal, H. Tagawa, and W. Lehnert, (The Electrochemical Society, Pennington NJ 1997), p. 1319.
59. S. Carter, A. Selcuk, R.J. Chater, J. Kajda, J.A. Kilner, and B.C.H. Steele, *Solid State Ionics*, **53–56**, 597 (1992).
60. J. Mizusaki, H. Tagawa, K. Tsuneyoshi, and A. Sawata, *J. Electrochem. Soc*., **138**, 1967 (1991).
61. T. Kenjo and M. Nishiya, *Solid State Ionics*, **57**, 295 (1992).
62. E.P. Murray, T. Tsai, and S.A. Barnett, *Solid State Ionics*, **110**, 235 (1998).
63. A. Hammouche, E. Siebert, and A. Hammou, *Mat. Res. Bull*., **24**, 367 (1989).
64. E. Siebert, A. Hammouche, and M. Kleitz, *Electrochim. Acta*, **40**, 1741 (1995).
65. M. Juhl, M. Mogensen, T. Jacobsen, BZachau-Christiansen, N. Thorup, and E. Skou, in *Solid Oxide Fuel Cells IV*, eds. M. Dokiya, O. Yamamoto, H. Tagawa, and S. C. Singhal (The Electrochemical Society, Pennington NJ, 1995), p. 554.
66. M. Odgaard and E. Skou, *Ionics*, **3**, 75 (1997).
67. P. Holtappels, M.J. Jørgensen, S. Primdahl, M. Mogensen, and C. Bagger, in *Proc. 3rd European Solid Oxide Fuel Cell Forum* ed. P. Stevens, p. 181 (1998).
68. M. Kertesz, I. Riess, D.S. Tanhauser, L. Langpape, and F.J. Rohr, *J. Solid State Chemistry*, **42**, 125 (1982).
69. A. Mackor, T.P.M. Koster, J.G. Kraaijkamp, and J. Gerretsen, in *Solid Oxide Fuel Cells (SOFCII)*, eds. F. Grosz, P. Zegers, S.C. Singhal, and O. Yamamoto (Commission of the European Communities, Luxemburg, L. EUR-13564-EN, 1991), p. 463.
70. E. Ivers-Tiffée, M. Schiessl, H.J. Oel, and W. Wersing, in *High Temperature Electrochemical Behaviour of Fast Ion and Mixed Conductors*, eds. F.W. Poulsen, J.J. Bentzen, T. Jacobsen, E. Skou, M.J.L. Østergård (Risø National Laboratory, Roskilde, Denmark, 1993), p. 69.
71. A. V. Virkar, K-Z. Fung, and S.C. Singhal, in *Ionic and Mixed Conducting Ceramics III*, eds. T. A. Ramanarayanan et al., Proc.Vol. 97-24 (The Electrochemcal Society Pennington, NJ, 1998), p. 113.
72. H. Tagawa, N. Mori, H. Takai, Y. Yonemura, H. Minamiue, H. Inaba, J. Mizusaki, and T. Hashimoto, in *Solid Oxide Fuel Cells V*, eds. U. Stimming, S. C. Singhal, H. Tagawa, and W. Lehnert (The Electrochemical Society, Pennington, NJ, 1997), p.785.
73. B. Zachau-Christiansen, T. Jacobsen, and S. Skaarup, *ibid*., p. 795.
74. J.H. Kuo and H.U. Andersen, *J. Solid State Chem*., **83**, 52 (1989).
75. I.G.K. Andersen, E.K. Andersen, P. Norby, and E. Skou, *J. Solid State Chem*., **113**, 320 (1994).
76. J.A.M. van Roosmalen, P. van Vlaanderen, and E.H.P. Cordfunke, *J. Solid State Chem*., **114**, 516 (1995).
77. J.F. Mitchell, D.N. Argyriou, C.D. Potter, D.G. Hinks, J.D. Jorgensen, and S.D. Bader, *Phys. Rev. B*, **54**, 6172 (1996).
78. S. Srilomsak, D.P. Schilling, and H.U. Anderson, in *Solid Oxide Fuel Cells (SOFC I)*, ed. S.C. Singhal, Proc. Vol. 89–10, (The Electrochemical Society, Pennington, NJ, USA, 1989), p.129.
79. M. Mori, Y. Heie, T. Yamamoto, and H. Itoh, *J. Electrochem. Soc*., **146**, 4041 (1999)
80. P. Norby, I.G.K. Andersen, and E.K. Andersen, *J. Solid State Chem*., **119**, 191 (1995)
81. T. Kawada, N. Sakai, H. Yokokawa, and M. Dokiya, *Solid State Ionics*, **50**, 189 (1992).
82. J.A.M. van Roosmalen and E.H.P. Cordfunke, *Solid State Ionics*, **52**, 303 (1992).
83. C. Clausen, C. Bagger, J.B. Bilde-Sørensen, and A. Horsewell, *Solid State Ionics*, **70**/**71**, 59 (1994).
84. G. Stocniol, E. Syskakis, and A. Naumidis, *J. Am. Ceram. Soc*., **78**, 929 (1995).
85. A. Mitterdorfer and L.J. Gauckler, *Solid State Ionics*, **111**, 185 (1998).
86. K. Wiik, C.R. Schmidt, S. Faaland, S. Shamsili, M.-A. Einarsrud, and T. Grande, *J. Am. Ceram. Soc*., **82**, 721 (1999).
87. F.W. Poulsen and N. van der Puil, *Solid State Ionics*, **53–56**, 89 (1992).